Journal of New Materials for Electrochemical Systems 19, 199-207 (2016)

Ethanol - Tolerant Oxygen Reduction Reaction of Non-Pt Catalysts in Alkaline Electrolyte

Chakkrapong Chaiburi*, Bernd Cermenek, Birgit Elvira Pichler, Christoph Grimmer, Alexander Schenk and Viktor Hacker

Institute of Chemical Engineering and Environmental Technology, Fuel Cell Systems Group, Graz University of Technology, NAWI Graz, Inffeldgasse 25C, 8010 Graz, Austria

Received: September 23, 2016, Accepted: October 24, 2016, Available online: December 10, 2016

Abstract: *Ag/C, Mn_3O_4/C and $AgMnO_2$/C electrocatalysts were selected for nanocatalyst structure and electrochemical activity characterisation by transmission electron microscopy (TEM), X-ray spectroscopy (EDX), cyclic voltammetry (CV), X-ray diffraction (XRD) and oxygen reduction reaction (ORR). The nanocatalysts displayed ethanol-tolerance for ORR in KOH solution electrolyte at different temperatures. All electrocatalysts prevented oxidation from ethanol crossover through the membrane from the anode to cathode compartments in alkaline direct ethanol fuel cells (ADEFCs). ORR results confirmed that $AgMnO_2$/C significantly improved the current activity.*

Keywords: Alkaline direct ethanol fuel cell, Oxygen reduction reaction, Ethanol-tolerant, Silver manganese oxides, Manganese oxides, Fuel cells

1. INTRODUCTION

Alkaline direct ethanol fuel cells (ADEFCs) are a fascinating option for applications as energy-converting equipment. They are alternative high energy density fuel cells and particularly useful as portable power sources. Fuel cells convert chemical energy from a fuel into electricity through a chemical reaction. They differ from batteries as they require a continuous source of fuel and oxygen or air to sustain the chemical reaction. The fuel comprises ethanol, an alkaline solution and air. Ethanol is economical and environmentally friendly with low market preparation [1] and no need of compression for storage and transfer [2]. It is oxidised at the anode side creating carbon dioxide and power by means of an electro-oxidation reaction. One advantage of ADEFCs is that they can operate at lower temperatures, however, a significant disadvantage is the high cost of platinum-based electrocatalysts [3]. Many researchers have investigated methods to reduce material cost and enhance the performance of the electrocatalyst. Performance loss for operational ADEFCs is caused by exposure to pollutants. The ethanol can crossover from the anode to the cathode side and becomes adsorbed on the surface of the electrocatalyst, thus blocking and preventing the adsorption of new oxygen atoms. Koscher and Kordesh [4] studied oxygen reduction reaction (ORR) on Pt and Ag electrocatalysts in 9 M KOH in the presence of methanol at 353 K. The Pt electrocatalyst displayed no significant drop in performance even at low methanol content, while the Ag electrocatalyst performed well at high methanol concentration. A mixed cathode of Ag catalyst with polytetrafluoroethylene (PTFE) as a hydrocarbon binder was examined to investigate the long-term effect at 343 K under oxygen atmosphere with Hg/HgO as a reference electrode [5]. Fang et al. synthesised a KMn_8O_{16} electrocatalyst by means of a one-step hydrothermal reaction. The quantity of electron exchange was 3.98 at 0.5 V vs. Hg/HgO. Under alkaline electrolyte in the presence of methanol, the KMn_8O_{16} catalyst displayed resistance towards methanol oxidation [6]. The reactions pathways of an alkaline direct ethanol fuel cell are shown below [7]:

Anode: $CH_3CH_2OH+12OH^- \rightarrow 2CO_2+9H_2O+12e^-$ $E^0 = -0.74V$

Cathode: $3O_2+6H_2O+12e^- \rightarrow 12OH^-$ $E^0 = 0.40V$

Over all reaction: $CH_3CH_2OH+3O_2 \rightarrow 2CO_2+3H_2O$ $E^0 = 1.24V$

Significant research regarding ADEFCs has explored non-noble metal electrocatalysts to reduce the expense of platinum-based catalytic materials and enhance ethanol-tolerance in the cathode.

*To whom correspondence should be addressed:
Email:kchakkrapong@yahoo.com; chakkrapong.chaiburi@student.tugraz.at
Phone: Fax: +43 (316) 873-8782

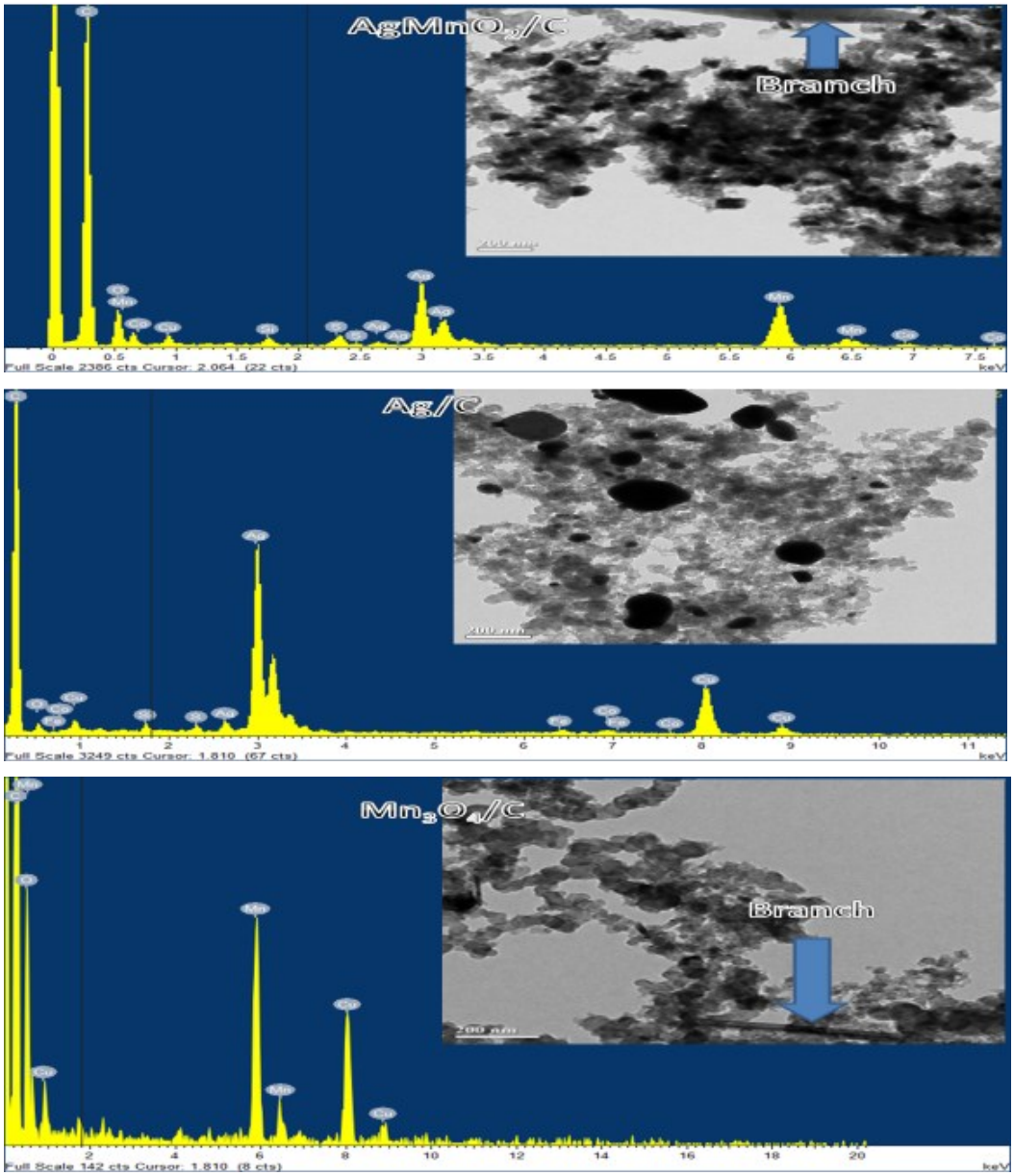

Figure 1. Transmission electron microscopy (TEM) and Energy-dispersive X-ray spectroscopy (EDX) for Ag/C, Mn_3O_4/C and $AgMnO_2$/C catalysts

According to the results, this study investigated Ag/C, Mn_3O_4/C and $AgMnO_2$/C catalysts in 0.1 M KOH solution with different ethanol-containing electrolytes at various temperatures.

2. EXPERIMENTAL

2.1. Synthesis of Catalyst Materials

2.1.1. Synthesis of Ag/C catalyst

A colloidal method was used to produce Ag/C [8]. A 20 wt % Ag/C catalyst was prepared from a mixture of 599 mg of trisodium citrate dehydrate (2.32×10^{-3} mol) and 69.3 mg $AgNO_3$ (4.08×10^{-4} mol) dissolved in 50 ml ultrapure water in the first beaker. The solution was blended until it was clear and then 15.5 mg of $NaBH_4$ (4.10×10^{-4} mol) was dissolved in 50 ml ultrapure water in the

Table 1. Summary of cyclic voltammetry parameters.

Procedure	Potential range (V) vs.RHE	Cycles	Scan rate (mV s^{-1})	Purge
Cleaning	0.20-1.40	10	50	N_2
Base CV	0.20-1.40	3	10	N_2
Banckground for ORR	0.20-1.20	2	10	N_2
Base CV	0.20-1.40	3	10	O_2
ORR*	1.20-0.20	2	10	O_2
ORR** (with 0.5MEtOH)	1.20-0.20	2	10	O_2
ORR** (with 1.0MEtOH)	1.20-0.20	2	10	O_2

*0, 400, 600, 900, 1200, 1600 and 2000 rpm, **0 and 1600 rpm

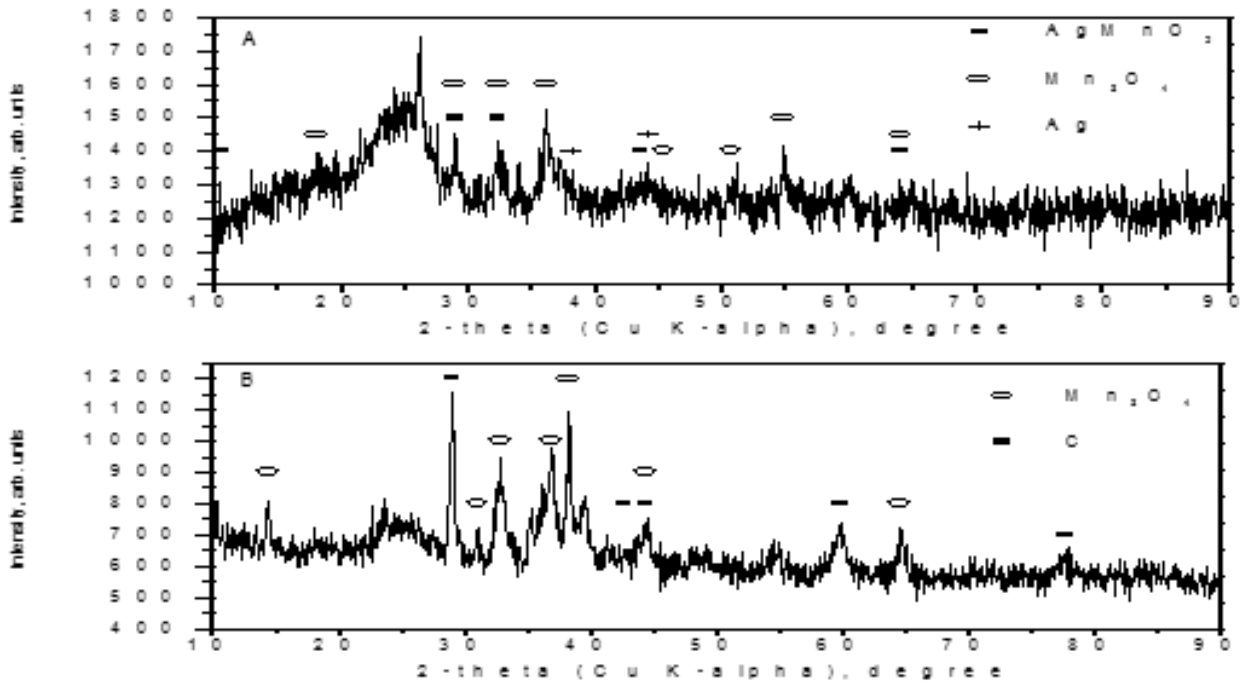

Figure 2. X-ray spectroscopy (XRD) for (A) $AgMnO_2$/C and (B) Mn_3O_4/C catalysts

second beaker. A droplet of $NaBH_4$ solution was added to the solution in the first beaker and the colloid solution displayed a yellowish-brown Ag nanomaterial. After 15-20 min, the entire $NaBH_4$ solution was gradually added to the quickly blended Ag solution which became dark brown. The Ag nanomaterial was then blended and scattered around for 15-30 min. Next, 176 mg of Vulcan XC-72R carbon black was scattered in 3 x 10^{-5} m^3 of ultrapure water with an ultrasonic probe for 10 min. This was added and stirred slowly to bond to the Ag nanoparticles and form the supported active nanomaterial. Ag was precipitated on the carbon black and the blend was mixed for 3h. The suspension was centrifuged at 11400 rpm for 10 min and ultrapure water was used twice to filtrate and wash the Ag molecules. The Ag/C catalyst was dried overnight in an oven at 363 K and the yield obtained was between 88% and 93%.

2.1.2. Synthesis of Mn_3O_4/C catalyst

Vulcan XC-72R 140 mg scattered in 300 ml of ethanol-water blended solution (8:2 v/v) was mixed to set up the MnO_2/C catalyst [8]. Then, 198 mg of $Mn(NO_3)_2{\times}4H_2O$ was added and mixed overnight at 333 K. Finally, the $Mn(NO_3)_2$/C was calcined at 673 K in a furnace for 2 h under N_2 atmosphere (heating rate of 278 K min^{-1}) to remove the slurry solvent.

2.1.3. Synthesis of $AgMnO_2$/C catalyst

A mixture of $AgNO_3$ and $KMnO_4$ (molar ratio of 1:1) was dissolved in ultrapure water at 353 K and acidified with a drop of 65% HNO_3 to obtain the $AgMn_xO_y$ catalyst [8-10] The solution was then gradually cooled to 273 K and the suspension precipitated as dark-blue needles. $AgMn_xO_y$ was filtrated, washed with iced ultrapure water and dried. Next, 462 mg of $AgMn_xO_y$ dissolved in 150 ml ultrapure water at 313-323 K was used to synthesize the $AgMnO_2$/C catalyst and Vulcan XC-72R carbon black was added. The black slurry was scattered with ultrasonic for 15 min. and then the water was gradually evaporated at a constant temperature of 333 K. Finally, the $AgMnO_2$/C was calcined in a tubular furnace for 2 h at 673 K under N_2 atmosphere with a heating rate of 278 K min^{-1}.

2.2. Characterization of the Catalyst Materials

Transmission electron microscopy (TEM) was used to determine the morphology of the Ag/C, Mn_3O_4/C and $AgMnO_2$/C catalysts and energy dispersive X-ray spectroscopy (EDX) measured the component compositions of all electrocatalysts. X-ray diffraction (XRD) was done using a X' Pert MPD, Philips diffractometer.

2.3. Electrode Preparation

In this research, electrochemical measuring techniques were conducted together with standard three-electrode configurations at different temperatures, such as 303, 313, 323 and 333 K, including 0.1 M KOH as alkaline electrolyte. A reference electrode was a reversible hydrogen electrode (RHE) and a platinum cathode was utilized as the counter electrode. The working electrode was a rotating disk electrode (RDE) with glassy carbon substrate. Regarding the impacts of various centralizations of EtOH, a reasonable amount was added into the working electrolyte (see Table 1). In addition, Nanopure water (18 MΩ-cm, Barnstead Nanopure) was used for setting up 0.1 M KOH and purity nitrogen (N_2) and oxygen (O_2) were also utilized. Moreover, Ag/C, Mn_3O_4/C and $AgMnO_2$/C were utilized as catalysts. The catalyst-loading on the tip of the working electrode (RDE) was 56 μg cm^{-2}. Electrochemical analyses were done from potentiostat/galvanostat as Autolab.

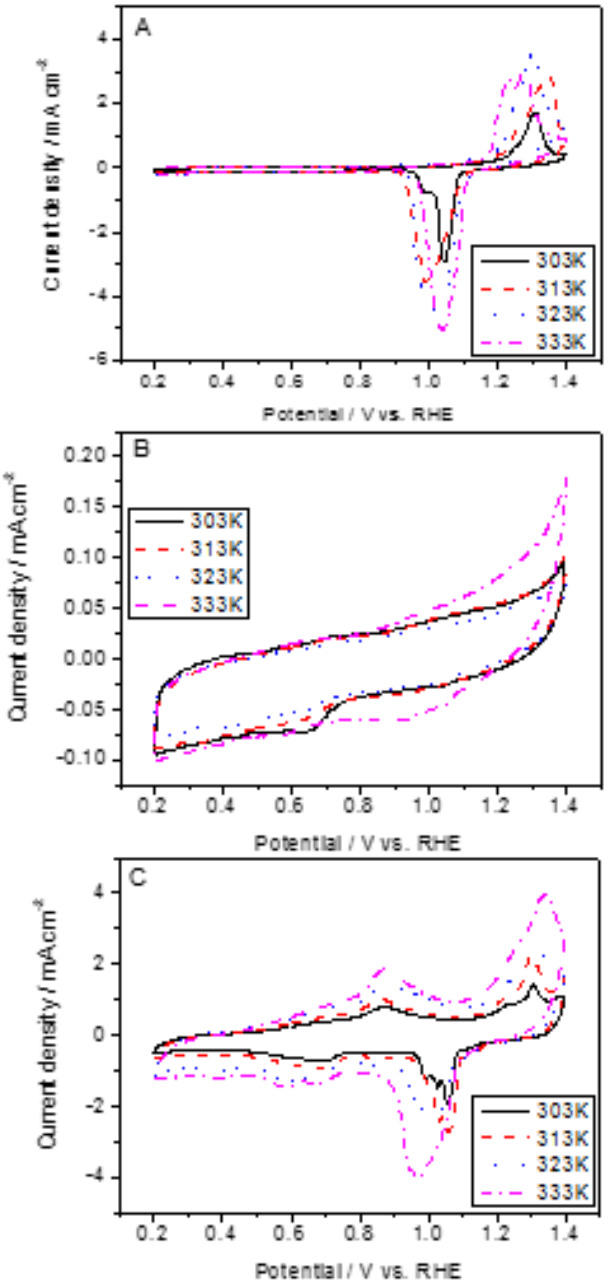

Figure 3. Cyclic voltammograms for the (A) Ag/C, (B) Mn_3O_4/C and (C) $AgMnO_2$/C catalysts in 0.1 M KOH with N_2 saturated at sweep rate 10 mV s^{-1} at 303, 313, 323 and 333 K.

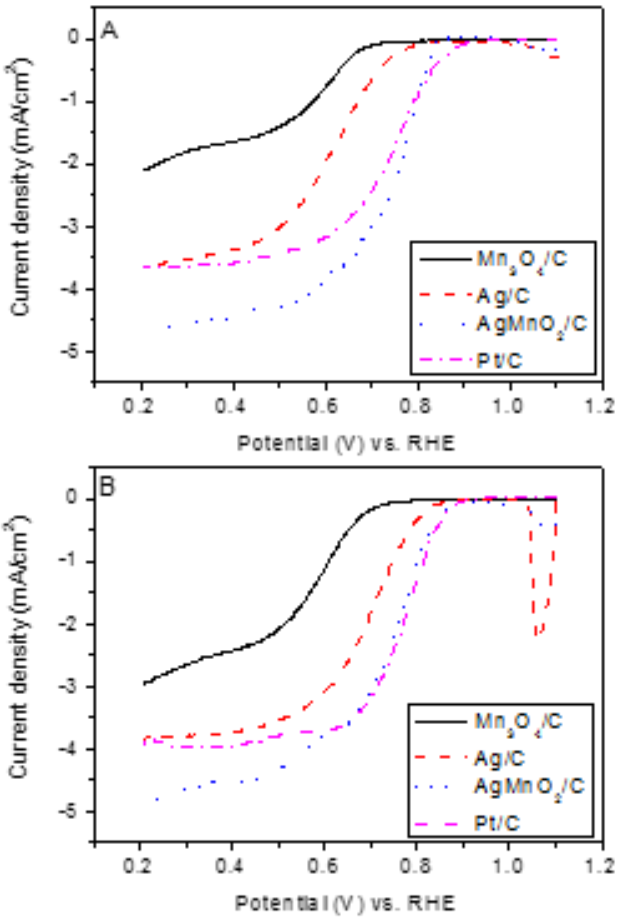

Figure 4. Linear potential scan curves of $AgMnO_2$/C, Mn_3O_4/C, Ag/C and Pt/C electrocatalysts on a rotating disk electrode (RDE) 0.1 M of KOH in O_2 saturated electrolyte at (A) 313 K and (B) 333 K, with a sweep rate of 10 mV s^{-1} and rotation rate of 1600 rpm.

2.4. Procedure

The experimental procedure for ORR at 303, 313, 323 and 333 K, as shown in Table 1.

3. RESULTS AND DISCUSSION

3.1. Physical characterization of Ag/C, Mn_3O_4/C and $AgMnO_2$/C electrocatalysts

Three morphologies, including dark spherical, gray spherical, and branch-like particles, were indicated by the transmission electron microscopy (TEM). The dark spherical particles ought to be Ag or Mn as metal and gray spherical particles as carbon black, while the branch-like particles were likely manganese oxides [11]. The EDX examination showed the majority of Ag and Mn metal, which were approx. 11.6% and 13.6%, respectively (Figure 1).

XRD peak of peak of $AgMnO_2$/C consisted Ag, $AgMnO_2$ and Mn_3O_4, with using JCPDS files no. 01-071-3762, 00-060-0300 and 01-075-1560, respectively. The diffraction spectra of Mn_3O_4/C contained carbon and Mn_3O_4, with using JCPDS files no. 01-071-4630 and 01-075-1560, respectively (Figure 2).

3.2. Electrochemical Measurements

3.2.1. Base cyclic voltammograms for the Ag/C, Mn_3O_4/C and $AgMnO_2$/C catalysts in 0.1 M KOH at 303, 313, 323 and 333 K

The CV curves showed Ag/C, Mn_3O_4/C and $AgMnO_2$/C electrocatalysts in N_2 saturation. A monolayer of Ag_2O was formed on the surface of RDE during the oxidation of Ag as shown in Figure 3A and 3C. In the bulk, AgOH and Ag_2O were formed [8]. The Ag

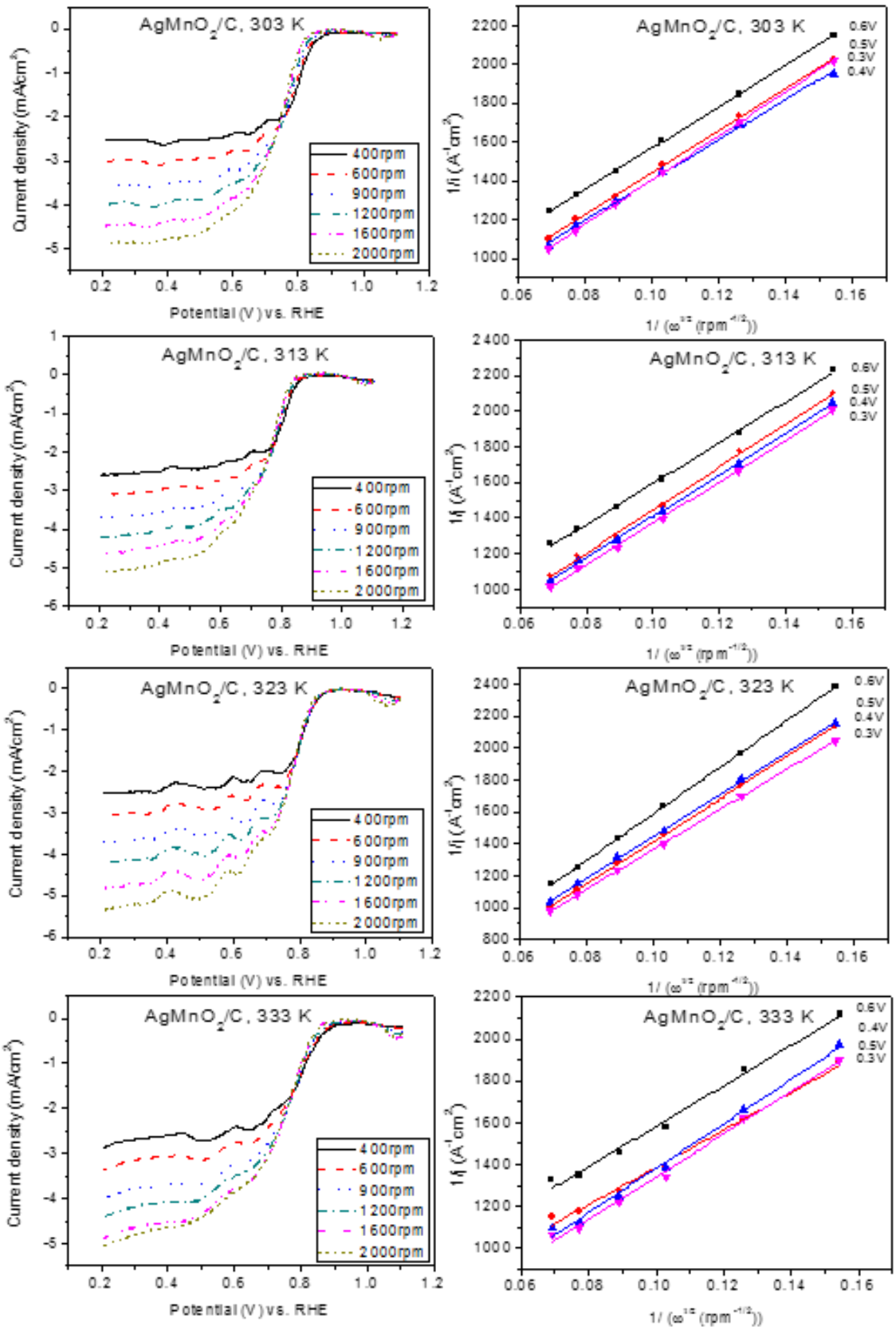

Figure 5. Oxygen reduction reaction potential scan curves of $AgMnO_2/C$ on rotating disk electrode in O_2 saturated 0.1 M KOH at 303, 313, 323 and 333 K with a sweep rate of 10 mV s^{-1}. Koutecky-Levich plots of $AgMnO_2/C$ at the different potential at 303, 313, 323 and 333 K.

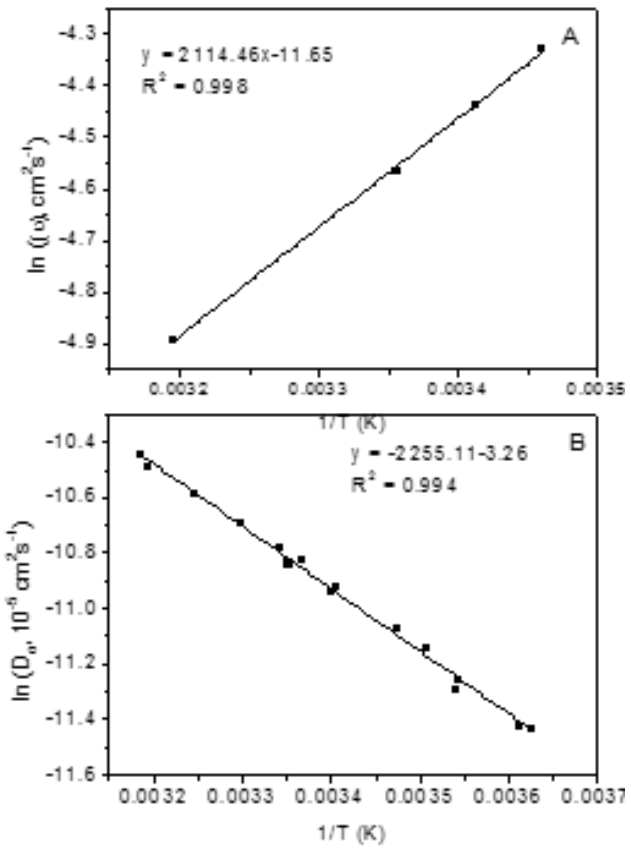

Figure 6. (A) Kinematic viscosity curve of the various temperatures and (B) Oxygen diffusion curve of the various temperatures

oxidation peak showed at potential 1.3V. The Mn_3O_4/C observed the peak of $Mn(OH)_2$ change to Mn_2O_3 and MnOOH at potential of about 0.7 V to 0.9 V, respectively (Figure 3B). The oxidation peak showed approximately 1.0 V as the oxidation of MnOOH to MnO_2. $AgMn_3O_4$/C electrocatalysts exhibited overlap of the oxidation peak of AgOH, Ag_2O and Mn_3O_4 [8]. The reduction peak of the $AgMn_3O_4$/C at 333 K was higher than the reduction peak at 303 K (see Figure 3C). The $AgMnO_2$/C electrocatalysts are believed to be advantageous for improving the ORR activity.

The initial ORR polarisation curve of the catalysts showed a well-defined diffusion-limiting current at E = 0.20-0.70 V, with potential between 0.70 < E < 0.90 V displayed in a region under mixed kinetic-diffusion control [12]. The performance of the $AgMnO_2$/C electrocatalyst was compared with the Pt/C electrocatalyst, which were found to be higher diffusion-limiting current at 313 K and 333 K (see Figure 4). These results are interesting since the $AgMnO_2$/C electrocatalyst is totally Pt-free. A comparison of the cost for the Ag-based electrocatalyst showed it to be much less than the Pt/C electrocatalysts.

3.2.2. Kinetic oxygen reduction for $AgMnO_2$/C catalysts in 0.1 M KOH at 303, 313, 323 and 333 K

The reduction of oxygen dissolved in KOH saturated solution as supporting electrolyte. The rotating disk electrode for different

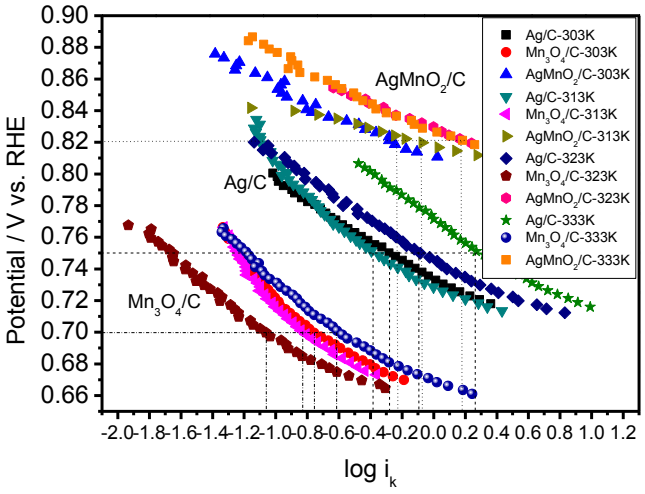

Figure 7. Tafel plots of oxygen reduction for Ag/C, Mn_3O_4/C and $AgMnO_2$/C electrocatalysts in 0.1 M KOH at temperatures of 303, 313, 323 and 333 K.

rotation rate of $AgMnO_2$/C electrocatalysts are shown in Figure 5. In each case, the most of oxygen reduction reaction curves obtained parallel curves. Koutecky-Levich curves for different potentials on the $AgMnO_2$/C electrocatalysts present linear and mostly parallel conducted from different rpm, which usually taken to imply first-order kinetics depending on oxygen and indicates the current is a diffusion controlled. The ORR can be represented by Koutecky-Levich Equation [14] as:

$$i^{-1} = i_k^{-1} + i_l^{-1} \quad (1)$$

$$i_l = 0.62nFAC_O D_O^{2/3} \nu^{-1/6} \omega^{1/2} \quad (2)$$

where i_l is the diffusion limiting current, n is the number of electrons transfer in the reduction of oxygen, F is the Faraday constant (96,485 C mol^{-1}), A is the geometric surface area of RDE (A = 1.96 x 10^{-5} m^2), C_O is the bulk concentration of the oxygen, D_O is the diffusion coefficient of the oxygen, n is the kinematic viscosity of the working electrolyte and w is the angular rotation rate of the electrode ($\omega = 2\pi f/60$) at 303, 313, 323 and 333 K [5, 13]. The value of n are collected from Chatenet and coworker at the different temperatures [15].

Table 2. The value of oxygen solubility (C_O), the value of oxygen diffusion (D_O) and the kinematic viscosities (n) at 303, 313, 323 and 333 K.

T, ºC	C_O, mol cm^{-3}	D_O, cm^2s^{-1}	n, cm^2s^{-1}
30	1.13×10^{-6}	2.24×10^{-5}	0.0093
40	1.03×10^{-6}	2.85×10^{-5}	0.0074
50	9.36×10^{-7}	3.56×10^{-5}	0.0060
60	8.58×10^{-7}	4.39×10^{-5}	0.0049

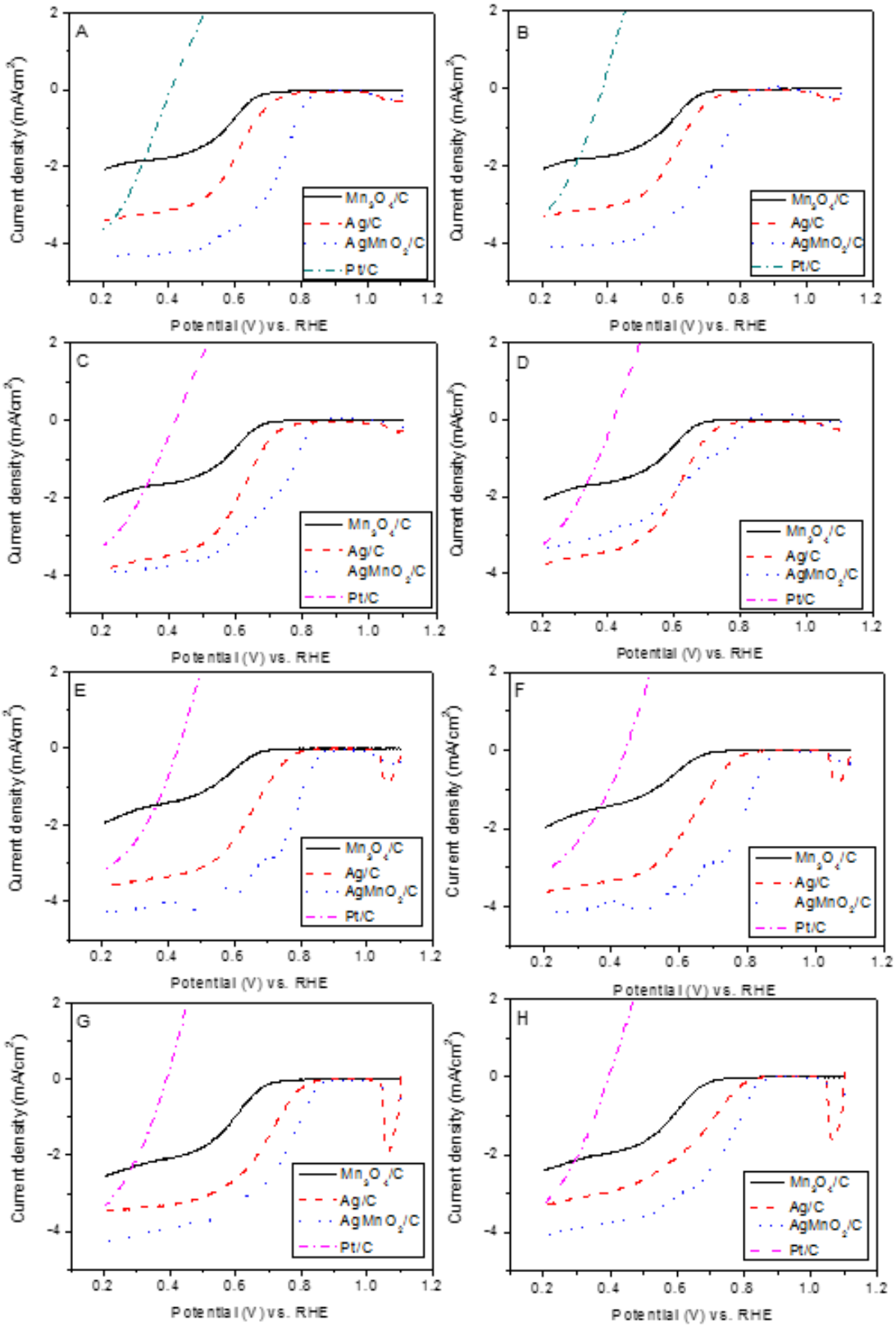

Figure 8. Linear potential scan curves of Pt/C, Ag/C, Mn_3O_4/C and $AgMnO_2$/C on rotating disk electrode in O_2 saturated : (A) 0.1 M KOH with 0.5 M EtOH at 303 K, (B) 0.1 M KOH with 1.0 M EtOH at 303 K, (C) 0.1 M KOH with 0.5 M EtOH at 313 K, (D) 0.1 M KOH with 1.0 M EtOH at 313 K, (E) 0.1 M KOH with 0.5 M EtOH at 323 K, (F) 0.1 M KOH with 1.0 M EtOH at 323 K, (G) 0.1 M KOH with 0.5 M EtOH and (H) 0.1 M KOH with 1.0 M EtOH at 333 K with sweep rate 10 mV s^{-1} and rotation rate 1600 rpm.

The collected data is calculated with the Arrhenius equation following [16]:

$$\nu = A\exp\frac{B}{T} \quad (3)$$

$$\ln\nu = \ln A - \frac{B}{T} \quad (4)$$

where ν is kinematic viscosities, A is a pre-exponential factor and B is the activation energy. The value of A is 8.72 x 10^{-6} cm^2 s^{-1} and B is 2114 K in 0.1M KOH (Eq. (4) and Figure 6A). The n values are shown in Table 2. The D_O is calculated from oxygen diffusion in KOH working electrolyte (approximate oxygen diffusion in H_2O = oxygen diffusion in KOH solution), shown in Figure 6B with the different temperatures [17]. The values are fitted curve with the Arrhenius equation (Eq. (5) and Figure 6B) [16].

$$\ln D_O = \ln A - \frac{B}{T} \quad (5)$$

The value of A is 3.83 x 10^{-2} cm^2 s^{-1} and B is -2255 K. As seen in Table 2, the value of D_O in KOH solution at different temperature. The value of C_O is determined from Eq. (6) [18].

$$K = \exp\{[0.046\ T^2+203.35\ T\ \ln(T/298) - (299.378+0.092T)(T-298) - 20.591x10^3]/8.3144\ T\} \quad (6)$$

$$c_{aq}=P_{O2}k \text{ or } c_{aq}/\ P_{O2} = k \quad (7)$$

where c_{aq} is mol of O_2/kg of H_2O, P_{O2} is pressure in atm and k is given by Eq. (6). Assumption of oxygen solubility (C_O) in H_2O is equal oxygen solubility (C_O) in KOH solution. The C_O, D_O and n values are shown in Table 2.

The information of each Koutecky-Levich curve determined number of electrons transfer from a slope of different catalysts at 0.3 V (see Table 3). The kinetic current i_k can be calculated by Eq. (8), where i_o is the observed current and i_d is the limiting current that can be obtained directly obtained from the ORR curve.

$$i_k = \frac{(i_d x i_o)}{(i_d - i_o)} \quad (8)$$

The number of electrons transfer are measured from different rotation speeds with Koutecky-Levich equation for $AgMnO_2$/C catalysts. The Koutecky-Levich curves exhibited good linear fitting for each potential of all catalyst. The number of electron transfer in 0.1 M KOH for $AgMnO_2$/C and Pt/C are n ≈ 4 at 303 K (Table 3). According to the value of oxygen solubility (C_O) and kinematic viscosities (n) are reduced. On the other hand, the value of oxygen diffusion (D_O) is increased at high temperature (see Table 2) [19].

The performance of the electrocatalysts is evaluated from kinetic current density (i_k), as seen in Figure 7. At temperature 333 K, all of electrocatalysts display higher mass activity than at temperature 303 K. The average Tafel slope for $AgMnO_2$/C, Ag/C, and Mn_3O_4/C are 39.17 mV dec^{-1}, 62.97 mV dec^{-1}, and 81.69 mV dec^{-1}, respectively.

3.2.3 Electrocatalytic activity towards oxygen reduction for Pt/C, Ag/C, Mn_3O_4/C and $AgMnO_2$/C electrocatalysts in 0.1 M KOH with various ethanol-containing electrolyte at 303, 313, 323 and 333 K

The effect of various ethanol-containing electrolytes on the performance of oxygen reduction on Pt/C working electrode is shown in Figure 8. The results of the linear potential scan curves on the surface of Pt/C electrocatalyst are exhibited the ethanol oxidation in the presence of ethanol.

The opposite way, other electrocatalyst as Ag/C, Mn_3O_4/C and $AgMnO_2$/C are ethanol-tolerant result for oxygen reduction reaction in the presence of different concentrations of ethanol. This confirms the result of the $AgMnO_2$/C electrocatalyst showing significantly enhancement of its ORR activity.

4. CONCLUSION

With the presence of ethanol in KOH electrolyte, the Ag/C, Mn_3O_4/C and $AgMnO_2$/C present ethanol-tolerant for oxygen reduction reaction. In this manner, in alkaline fuel cells, all electrocatalysts keep an ethanol oxidation reaction from ethanol crossover at the cathode side. Most consequences of ORRs affirm that the $AgMnO_2$/C fundamentally changes the present activity.

REFERENCES

[1] J. Huang, A. Faghri, J. Fuel Cell Sci. Technol., 11, 051007 (2014).
[2] J. Kemsley, Chem. Eng. News, 85, 55 (2007).
[3] M. Zhiani, H.A. Gasteiger, M. Piana, S. Catanorchi, Int. J. Hydrogen Energy, 36, 5110 (2011).
[4] G. Koscher, K. Kordesch, J. Power Sources, 136, 215 (2004).
[5] N. Wagner, M. Schulze, E. Gülzow, J. Power Sources, 127, 264 (2004).

Table 3. Comparison of the total number of electrons transfer (n) and the kinetic current activity (i_k) determined by RDE at 0.3 V, 1600 rpm, 0.1 M KOH.

Temperature, °C	n @ 0.3V				i_k			
	Ag/C	Mn_3O_4/C	$AgMnO_2$/C	Pt/C	Ag/C	Mn_3O_4/C	$AgMnO_2$/C	Pt/C
30	3.28	3.00	3.81	3.70	1.14	0.48	0.63	0.52
40	3.28	2.76	3.38	3.00	0.78	0.39	1.05	1.16
50	2.71	2.71	2.86	2.59	1.63	0.24	1.68	1.13
60	2.33	2.54	2.25	2.25	1.31	0.66	1.28	1.94

[6] Y. Fang, X. Yang, L. Wang, Y. Liu, J. Power Sources, 267, 33 (2014).
[7] A.D. Modestov, M.R. Tarasevich, A.Y. Leykin, V.Y. Filimonov, J. Power Sources, 188, 502 (2009).
[8] Q. Tung, L. Jiang, J. Qi, Q. Jiang, S. Wang, G. Sun, Appl. Catal.: B Environ., 104, 337 (2011).
[9] Q. Wu, L. Jiang, L. Qi, L. Yuan, E. Wang, G. Sun, Electrochimica Acta, 123, 167 (2014).
[10]C. Grimmer, R. Zacharias, M. Grandi, B. Pichler, I. Kaltenboeck, F. Gebetsroither, J. Wagner, B. Cermenek, S. Weinberger, A. Schenk, V. Hacker, J. Electrochem. Soc., 163, 278 (2016).
[11]W. Sun, A. Hsu, R. Chen, J. Power Sources, 196, 627 (2011).
[12]Y. Garsany, S. Dutta, K.E. Swider-Lyons, J. Power Sources, 216, 515 (2012).
[13]J. Qiao, L. Xu, L. Ding, P. Shi, L. Zhang, R. Baker, J. Zhang, Int. J. Electrochem. Sci., 8, 1189 (2013).
[14]H. Meng, P. K. Shen, Electrochem. Commun., 8, 588 (2006).
[15]M. Chatenet, M. B. Molina-Concha, N. El-Kissi, G. Parrour, J. P. Diard, Electrochimica Acta, 54, 4426 (2009).
[16]A.C. Garcia, J.J. Linares, M. Chatenet, E.A. Ticianelli, Electrocatalysis, 5, 41 (2014).
[17]P. Han, D. M. Bartels, J. Phys. Chem., 100, 5597 (1996).
[18]D. Tromans, Ind. Eng. Chem. Res., 39, 805 (2000).
[19]W. Xing, G. Yin, J. Zhang, "Rotating Electrode Methods and Oxygen Reduction Electrocatalysts", Amsterdam: Elsevier; 2014.